"Physics of Auroral Phenomena", Proc. XXIX Annual Seminar, Apatity, pp. 31-35, 2006

Polar Geophysical Institute

NUMERICAL MODELING OF AURORAL ELECTROJET DURING GEOMAGNETIC DISTURBANCES

M.V. Klimenko[1], V.V. Klimenko[2], V.V. Bryukhanov[1]

[1]*State Technical University, Kaliningrad, 236000, Russia*
[2]*West Department of IZMIRAN, Kaliningrad, 236017, Russia, wwk@izmiran.koenig.su*

Abstract. Numerical modeling of auroral electrojet behavior during geomagnetic disturbances has been performed based on the Global Self-consistent Model of Thermosphere-Ionosphere-Protonosphere system (GSM TIP) developed at WD IZMIRAN. The simulation comprises not only the traditional blocks of the model, such as the thermosphere, lower ionosphere, F-region of the ionosphere, external ionosphere and protonosphere in which the key parameters of the near-Earth thermal plasma are calculated. A new feature is that instead of calculation of the electric fields of a dynamo and magnetosphere origin, a new block is added, in which along with calculation of spatial distribution of large-scale electric field potential, the calculation of zonal current density in the ionosphere is included. In the old version of the model the 3D current continuity equation in the ionosphere was reduced to the 2D equation by integration over the height of the current-carrying ionosphere layer with the subsequent numerical integration of the resulting elliptic-type partial derivative equation. In the new model this integration is performed along the geomagnetic field lines laying in the current-carrying layer of the ionosphere. Within this modified model, the effect of Region 1 field aligned current enhanced during geomagnetic disturbances, as well as polar cap potential drop difference (which are model inputs), in the auroral electrojet distribution is calculated. Both quasi-stationary solutions and time evolution of the auroral electrojet during geomagnetic disturbances are obtained. It is shown that the simulation results are in rather a good qualitative and quantitative agreement with the observations.

Introduction

During geomagnetic disturbances there is an amplification of electric fields and currents in a high-latitude ionosphere. These fields cause electromagnetic drifts of thermal plasma in F-region of ionosphere which result in change of its density. Besides, the electric fields and currents will penetrate from a high-latitude ionosphere to the average and low latitudes. Thus, the present work is also devoted to numerical modeling of these processes.

Model

The results of the calculations executed on the modified model GSM TIP developed in WD IZMIRAN (Namgaladze et al., 1988) in which the block of calculation of electric fields is changed are submitted. In the new block the decision of the 3D equation of preservation of density of a full current in the Earth's ionosphere is carried out by its reduction to 2D by integration not on height of a current-carrying layer of the ionosphere as it had been earlier, but along the pieces of geomagnetic field lines laying in a current-carrying layer. Besides, in the new block the distribution of linear and surface density of a zonal current in the ionosphere are calculated.

The calculations were carried out self-consistently for equinoctial conditions (March 22, 1987) at low solar activity ($F_{10.7} = 76$).

Results and Discussion

In Fig. 1 the designed distribution in the northern and southern polar caps of potential of the electric field generated both by magnetosphere sources, and ionosphere dynamo is shown. In this variant field aligned currents of Region 1 at geomagnetic latitudes $\Phi = \pm 75°$, equal $5 \cdot 10^{-8}$ A/m^2 for quiet conditions (above) and $2 \cdot 10^{-7}$ A/m^2 for disturbed (below) and field aligned currents of Region 2 at geomagnetic latitudes $\Phi = \pm 70°$, equal $3 \cdot 10^{-8}$ A/m^2 for quiet conditions and $1.2 \cdot 10^{-7}$ A/m^2 for the disturbed ones were set. Thus, the potential drop through a polar cap in quiet conditions makes 18 kV in the northern hemisphere and 12 kV in southern, and in the disturbed conditions – respectively 93 kV and 54 kV.

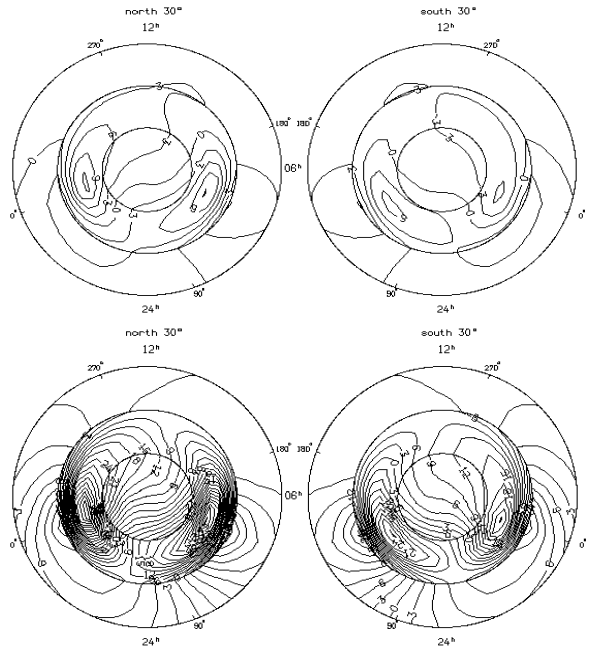

Fig. 1. Distribution of the electric field potential in the northern (on the left) and southern (on the right) polar caps at the set field aligned currents of Region 1 and 2 in quiet (above) and disturbed (below) conditions.

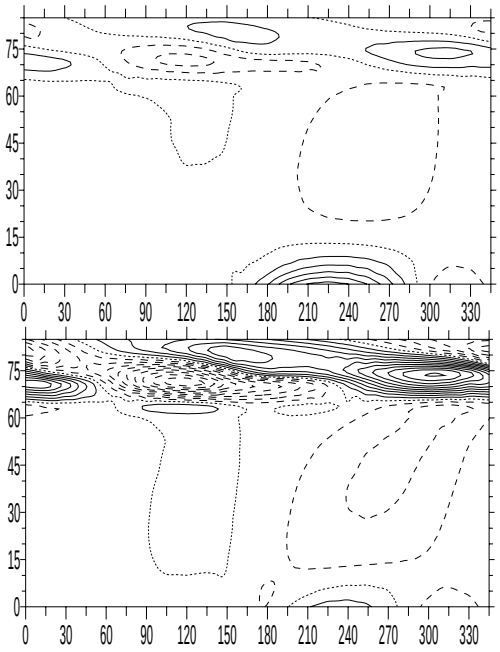

Fig. 2. Distribution of linear density of a zonal current, positive in the east direction in the Cartesian geomagnetic coordinate system longitude – latitude, corresponding to the distribution of potential submitted in Fig. 1.

In Fig. 2 the designed distribution of linear density of a zonal current, positive in the eastern direction, in the Cartesian geomagnetic coordinate system longitude – latitude for quiet (top) and disturbed (bottom) conditions, respectively, there is shown a distribution of the electric field potential, shown on Fig. 1. Continuous, shaped and dotted lines hereinafter show positive, negative and zero currents respectively. The step between neighboring isolines is 5 A/km. It is evident, that in quiet conditions the linear density of auroral electrojet makes ~10 A/km, the eastward equatorial electrojet ~25 A/km and westward ~5 A/km. In the disturbed conditions the linear density of auroral electrojet grows up to ~50 A/km whereas the density of eastward equatorial electrojet decreases up to ~10 A/km at constant westward electrojet on equator. Thus, Harang discontinuity is displaced slightly in the evening sector. In the disturbed conditions the penetration of eastward current to equator in the morning sector of local time and westward from evening to dayside takes place, that, apparently, results in reduction of density of the eastward equatorial electrojet in the given variant of calculations (at the set of field aligned currents).

In Fig. 3 the distribution of the electric field potential in polar caps at specified on geomagnetic latitudes $\Phi = \pm 75°$ a potential drop through the polar caps, equal 40 kV for quiet conditions (top) and 120 kV for disturbed (bottom) and specified on geomagnetic latitudes $\Phi = \pm 70°$ field align currents of Region 2 equal $3 \cdot 10^{-8}$ A/m^2 for quiet conditions and $2 \cdot 10^{-7}$ A/m^2 for the disturbed is shown. It is evidently, that at the setting of the potential drop through the polar caps in the disturbed conditions the potential distribution becomes four-cellular as against two-cellular in quiet conditions.

In Fig. 4 the distribution in the northern hemisphere of linear density of a zonal current for the variant of calculation presented in Fig. 3 is shown. It is evident, that in quiet conditions the linear density of eastward auroral electrojet makes ~30 A/km, westward ~10 A/km, eastward equatorial electrojet ~45 A/km and westward ~10 A/km. In the disturbed conditions the linear density of the eastward auroral electrojet grows up to ~105 A/km, westward up to ~60 A/km, the density of eastward equatorial electrojet grows up to ~50 A/km, and the westward – decreases up to ~5 A/km. Thus, Harang discontinuity, as well as in the previous case, is displaced slightly in the evening sector. In the disturbed conditions the penetration of the eastward current from the auroral zone to the equator in the evening-night sector of the local time takes place, which, apparently, results in the reduction of density of the westward equatorial electrojet and amplification of the eastward one in the given variant of calculations (at the setting of the potential drop through polar caps).

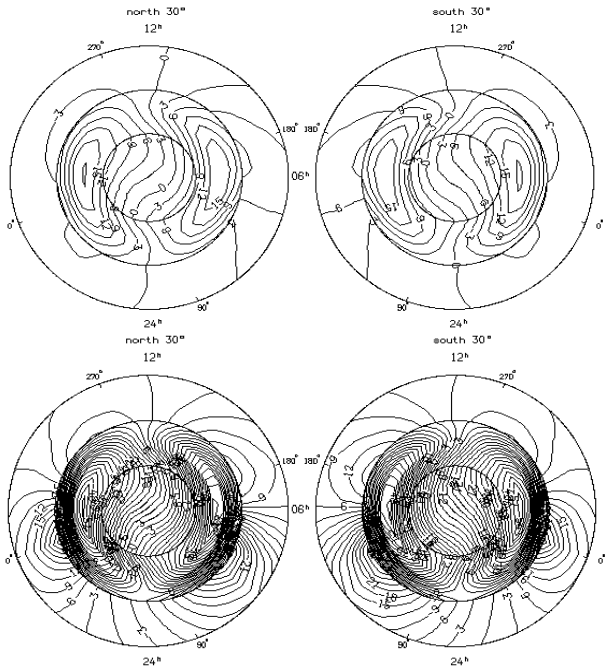

Fig. 3. The same, as in Fig. 1, at the setting of the potential drop through polar caps and field aligned currents of Region 2.

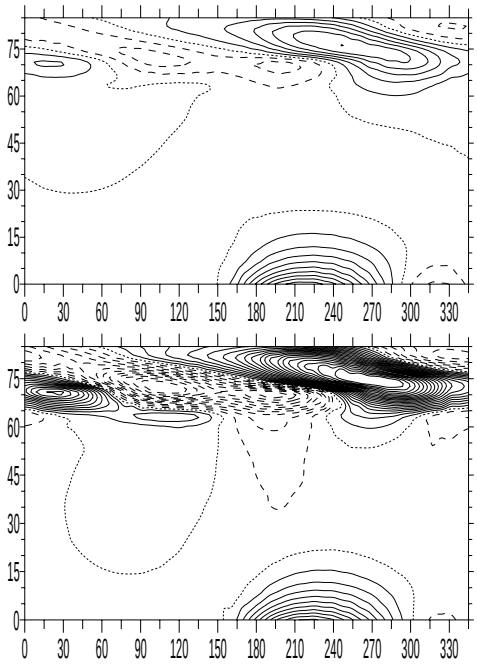

Fig. 4. The same, as in Fig. 2, corresponding to the distribution of potential presented in Fig. 3.

Fig. 5 shows the model of a substorm used in our calculations, where the change concerning UT of potential drop through polar caps (at the left) and field aligned currents of Region 2 (on the right) are presented. The growth phase of a substorm of 30 minutes duration is replaced with a phase of restoration. The duration of a modeling substorm is 4 hours.

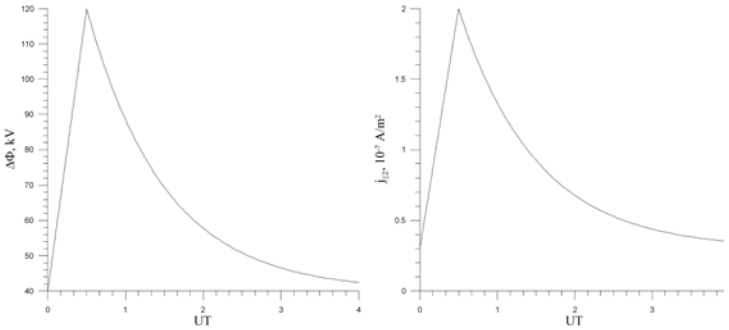

Fig. 5. The variation of UT potential drop through the polar caps (in the left panel) and field aligned currents of Region 2 (in the right panel) during a modeling substorm.

In Fig. 6 the designed distributions in the northern hemisphere of linear density of a zonal current in quiet conditions (the left panel) and during a substorm (the right panel) at 00.30 UT, 01.00 UT, 01.30 UT and 02.00 UT, and in Fig. 7 - at 02.30 UT, 03.00 UT, 03.30 UT and 04.00 UT are shown (the distribution of the linear density of a zonal current at 00.00 UT, that is at the moment of the beginning of a substorm, is shown in Fig. 4 above). The distribution of the linear density of a current at the end of a growth phase practically coincides with the one presented above in Fig. 4 below. At the recovery phase of substorm the currents in the auroral zone decrease. At the same time, during some time moments (in 1.5 and 2.5 hours after the beginning of a substorm) the easing of the eastward equatorial electrojet takes place. Since the basic source of equatorial electrojet is the thermosphere wind, apparently, the substorm generates waves in the neutral atmosphere, resulting in such changes of currents at the equator.

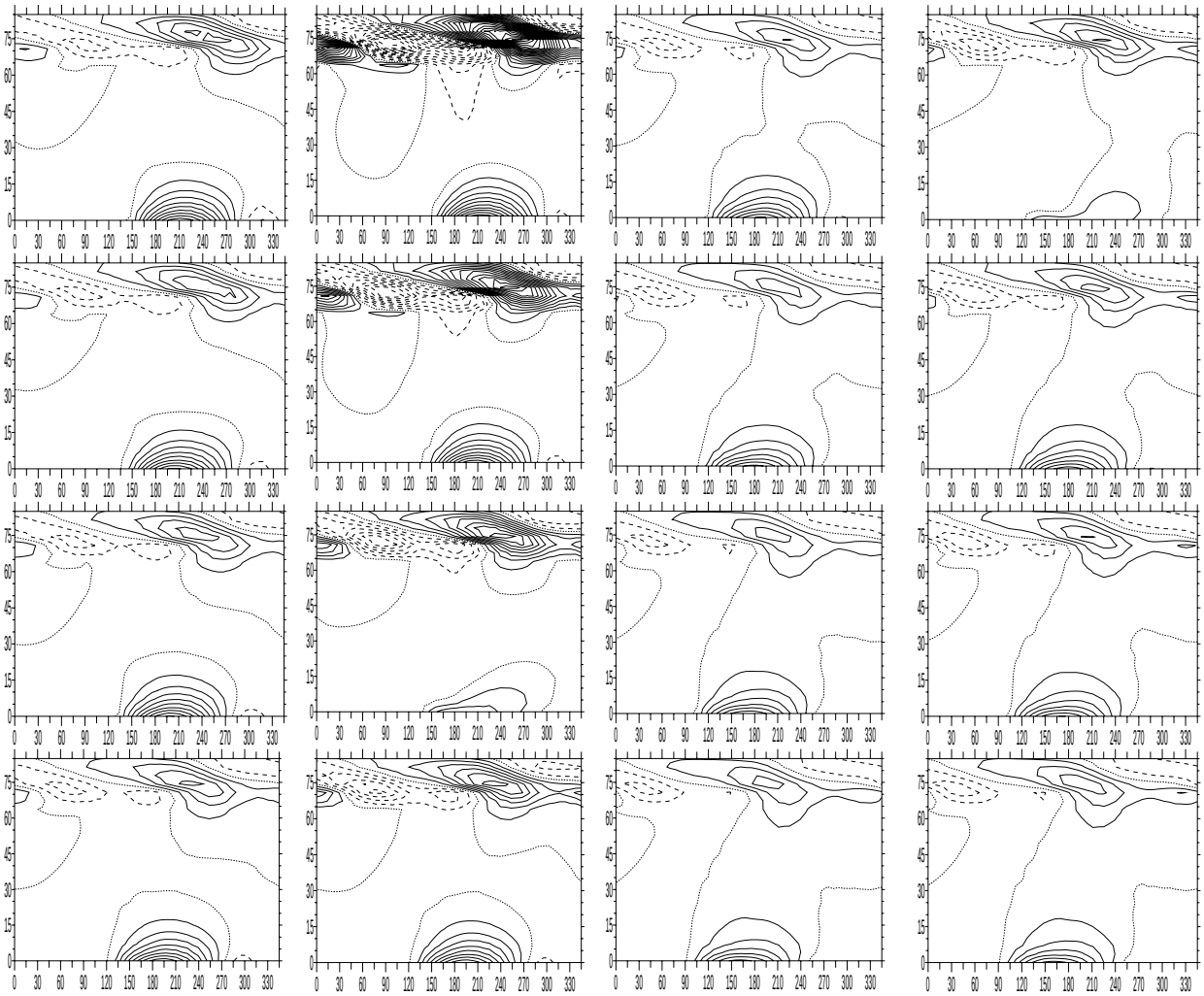

Fig. 6. The designed distributions in the northern hemisphere of linear density of a zonal current in quiet conditions (the left panel) and during a substorm (the right panel) at 00.30 UT, 01.00 UT, 01.30 UT and 02.00 UT (from top to bottom).

Fig. 7. The designed distributions in the northern hemisphere of linear density of a zonal current in quiet conditions (the left panel) and during a substorm (the right panel) at 02.30 UT, 03.00 UT, 03.30 UT and 04.00 UT (from top to bottom).

It is necessary to note, that according to experimental data (Kamide, 1991) the Harang discontinuity, which is defined as a border between the eastward and westward auroral electrojets or a border between the areas with northward and southward electric fields during substorms is shifted in the evening sector that will be coordinated with the results of calculations we have obtained (Fig. 2, 4). Besides, during a substorm there is a much greater growth of the westward electrojet, than of the eastward one, that is connected with the growth of conductivity of the ionosphere during a substorm, the greatest in the region of the westward electrojet. As in our substorm model there is no change of conductivity of the ionosphere due to precipitation of high-energy particles, we have received an opposite pattern of the behavior of auroral currents. An important conclusion that for the correct description of electrodynamics of a high-latitude ionosphere during substorms it is necessary to take into account the precipitations of high-energy particles in the auroral zone follows from this.

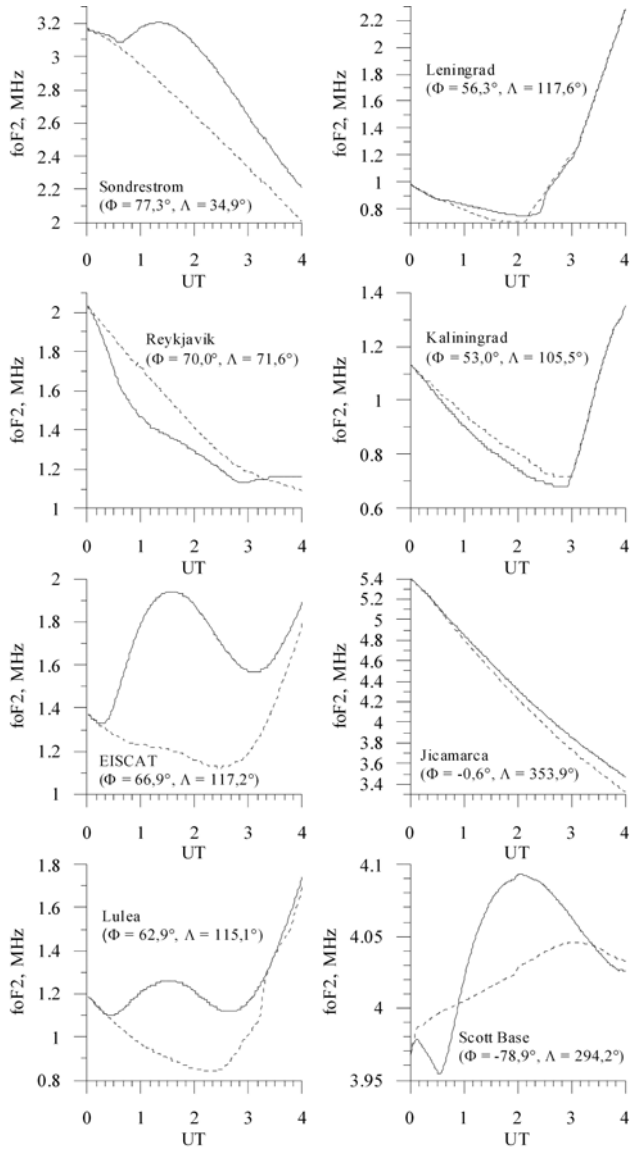

Fig. 8. The designed development on UT critical frequency of a F2-layer of an ionosphere, foF2, in quiet conditions (dotted curves) and during a substorm (continuous curves) for various stations.

The calculations of all key parameters of the near-Earth environment for 19 separate stations in both hemispheres, mainly the high-latitude ones had been carried out. The most interesting results for 8 of them are presented in Fig. 8, which shows a quiet (shaped lines) and a 0disturbed (continuous lines) development in UT critical frequency of the F2-layer of the ionosphere, foF2, for the stations of Sondrestrom (Greenland), Reykjavik (Iceland), EISCAT (Norway), Lulea (Sweden), Leningrad (Russia), Kaliningrad (Russia), Jicamarca (Peru) and Scott Base (Antarctica). One can see the distinction of the effects caused by a substorm at various stations. So, for example, at stations of Reykjavik and EISCAT, taking place during a substorm in the morning sector and insignificantly differing on the geomagnetic latitude the disturbances have a different sign – in Reykjavik there are negative disturbances, and in EISCAT – positive. A similar situation takes place at two middle-latitude stations, the Leningrad and Kaliningrad ones, differing from each other insignificantly on geomagnetic latitude and taking place approximately in one longitudinal sector. At the station of Leningrad the modeling substorm results in a positive disturbance of the foF2, which more than two hours after the beginning of a substorm is replaced with negative whereas at the station of Kaliningrad a negative disturbance takes place. At the equatorial station of Jicamarca we see a small positive disturbance, and at the Antarctic station of Scott Base a negative disturbance is replaced with a positive one, which then becomes negative. To explain these effects of a substorm in foF2 it is not enough to involve the local processes but it is necessary to consider existential distribution of all parameters of the near-Earth plasma.

Summary

Thus, it is shown, that the given model can describe the distribution of the potential of the electric field and currents in the ionosphere of the Earth both in quiet conditions, and during disturbances. Results of the carried out calculations specify that during the disturbances currents in the auroral ionosphere influence the equatorial electrojet. It is noted also, that for the correct description of variations of currents during substorms it is necessary to take into account the necessary precipitation of high-energy auroral particles.

References

Kamide, Y., The Auroral Electrojets: Relative Importance of Ionospheric Conductivities and Electric Fields, *Auroral Physics, Ed. C.-I. Meng, M.J. Rycroft and L.A. Frank,* 385-399, 1991.

Namgaladze A.A., Yu.N. Korenkov, V.V. Klimenko, I.V. Karpov, F.S. Bessarab, V.A. Surotkin, T.A. Glushchenko and N.M. Naumova, Global Model of the Thermosphere–Ionosphere–Protonosphere System, *Pure and Appl. Geophys. (PAGEOPH*), *127*, № 2 / 3, 219-254, 1988.